PCCP

Travelling waves in the Oregonator model for the BZ reaction

I. Z. Kiss,[a] J. H. Merkin,[a] S. K. Scott[b] and P. L. Simon[c]

[a] *Department of Applied Mathematics, University of Leeds, Leeds, UK LS2 9JT*
[b] *Department of Chemistry, University of Leeds, Leeds, UK LS2 9JT*
[c] *Department of Applied Analysis, Eötvös Loránd University, Budapest, Hungary*

Received 21st July 2003, Accepted 16th October 2003
First published as an Advance Article on the web 7th November 2003

Numerical solutions of the travelling wave equations that arise in the two-variable Oregonator model for the BZ reaction are obtained for a wide range of parameter values. The main feature is the saddle-node bifurcation in the solutions, giving upper bounds for the existence of travelling waves and indicating the change from the excitable to the subexcitable regimes. The values of the upper bound f_m of the stoichiometry factor f in the model are determined in terms of the excitability parameter ε for various values of the kinetic parameter q and D, the ratio of the diffusion coefficients of $HBrO_2$ and the oxidized form of the catalyst.

1 Introduction

Propagating pulses of reaction are basic to many spatially distributed chemical or biological systems and, in particular, are an important feature of excitable media. In these systems the pulse consists of a rapid reaction, the 'excitory region', followed by a much slower recovery to its original state. During the recovery stage the system is refractory, being insensitive to further stimuli. As a result, excitable systems subject to external stimuli above the threshold required to excite the medium usually form single pulses or trains of equally spaced waves (target patterns). The excitable media, perhaps, studied in most detail, both experimentally and theoretically, are based on the Belousov–Zhabotinsky (BZ) reaction. The excitability of the BZ reaction was predicted originally by Field and Noyes[1] and later confirmed experimentally.[2] As well as being of interest in their own right, these systems are also used as paradigms for the more complex excitable media that arise in the biological context.

Models for BZ systems are often based on Oregonator kinetics,[3,4] which involve the three active species, an autocatalyst $HBrO_2$, an inhibitor Br^- and an oxidised form of the catalyst M_{ox}. Expressing this mechanism in dimensionless form[5,6] shows that, to a good approximation, the concentration of Br^- can be regarded as varying quasi-statically in relation to the concentrations of the other two active species. In this reduced, two-variable form, the reaction dynamics are relatively simple. There is only one (chemically acceptable) steady state, with parameter values for which this is an excitable state. There is also the possibility of oscillatory behaviour arising from Hopf bifurcations. This two-variable reaction mechanism has been used extensively as the kinetics in models of spatially-distributed systems,[7] both as a generic model for excitable media and, more directly, to describe specific effects seen in BZ systems (effects of electric fields[8–10] and differential illumination on a light sensitive version of the BZ reaction[11–14] are two such examples).

Even though this kinetic model has been used very widely for spatially distributed systems, one aspect that has not been treated fully is basic and concerns the travelling waves that can arise in the model. These are waves, constant in form, propagating with a constant speed and dependent only on a single travelling co-ordinate. The problem lies in obtaining reliable numerical solutions to the ordinary differential equations that describe these waves. The main difficulty of which is having to account accurately for the very different length scales of the excitory and recovery regions. Progress towards understanding travelling wave solutions has been restricted to asymptotic limits[15–17] and to piecewise-linear representations of the kinetics.[18,19] For the Oregonator scheme, the asymptotic solutions are derived in the limit as $\varepsilon \to 0$, where the parameter ε (see the model described below) can be regarded as a measure of the excitability of the system, and give the wave speed in this limit.

Recently we have derived a reliable numerical algorithm for solving travelling wave equations, which can have very different length scales for the reaction zones.[20–22] This method was developed originally for a series of combustion problems, where the wave structure can have a qualitatively similar form to that arising in the Oregonator model for the BZ reaction. We have been able to adapt this technique successfully to deal with the BZ system and we are able to determine numerical solutions to the travelling wave equations for this system over a wide range of parameter values.

A significant feature that emerges clearly from our numerical solutions is the limit on the existence of waves for non-zero values of ε; the asymptotic solution for $\varepsilon \to 0$ does not provide such an upper bound. This effect has been recognised in numerical solutions of corresponding initial-value problems and has been referred to as the system becoming 'subexcitable'.[13,14] At this parameter boundary the system changes from being excitable, where above-threshold inputs lead to propagating pulses, to subexcitable, where there is propagation failure. This effect has also been observed in experiments on light-sensitive versions of the BZ reaction.[13,23] The behaviour of this excitable boundary has not previously been fully mapped out in parameter space. Our numerical scheme allows us to do this with this boundary then being seen as arising from a saddle-node bifurcation in solutions to the travelling wave equations. So the change from excitable to subexcitable is seen as an 'extinction' effect with an abrupt change in nature between these regimes.

2 Equations

In the Tyson–Fife dimensionless variables the two-variable Oregonator model in a one-dimensional spatially distributed

 DOI: 10.1039/b308315b

system leads to the equations

$$\frac{\partial u}{\partial t} = \frac{\partial^2 u}{\partial x^2} + \frac{1}{\varepsilon}\left(u(1-u) - \frac{fw(u-q)}{u+q}\right) \quad (1)$$

$$\frac{\partial w}{\partial t} = D\frac{\partial^2 w}{\partial x^2} + u - w \quad (2)$$

where $D = \dfrac{D_w}{D_u}$ (ratio of diffusion coefficients) and the other parameters are the standard Oregonator parameters, see refs. 5–7,24 for example. In eqns. (1) and (2), u and w are dimensionless concentrations of $HBrO_2$ and M_{ox}, respectively. This model assumes that v, the dimensionless concentration of Br^-, varies quasi-statically with u and w as

$$v = \frac{fw}{u+q}$$

To obtain the corresponding travelling wave equations we introduce the travelling co-ordinate $y = x - ct$, where c is the (constant) wave speed (without any loss in generality we can assume that $c \geq 0$), and look for a solution in the form $u = u(y)$, $w = w(y)$. This results in the travelling wave equations

$$u'' + cu' + \frac{1}{\varepsilon}\left(u(1-u) - \frac{fw(u-q)}{u+q}\right) = 0 \quad (3)$$

$$Dw'' + cw' + u - w = 0 \quad (4)$$

(where primes denote differentiation with respect to y). The boundary condition is (for a single pulse)

$$(u, w) \to (u_s, w_s) \quad \text{as } |y| \to \infty \quad (5)$$

where (u_s, w_s) is the steady state of the kinetic system, given by

$$u_s = w_s = \frac{1}{2}\left(1 - f - q + \sqrt{(1-f-q)^2 + 4q(f+1)}\right) \quad (6)$$

Before examining the solutions to the travelling wave eqns. (3)–(5), it is useful to consider briefly the temporal stability of the kinetic system. If we put $u = u_s + U$, $w = w_s + W$ and linearize the kinetic equations (essentially eqns. (1) and (2) without the spatial derivative terms), we obtain the linear system

$$\frac{dU}{dt} = \frac{1}{\varepsilon}(\alpha U - \beta W), \quad \frac{dW}{dt} = U - W \quad (7)$$

where

$$\alpha = 1 - 2u_s - \frac{2fqu_s}{(u_s+q)^2}, \quad \beta = \frac{f(u_s - q)}{(u_s + q)}$$

Note that $\beta > 0$ and, for any values of the parameters, $\beta - \alpha > 0$. A solution of eqn. (7) in the form $(U, W) \propto e^{\lambda t}$ leads to an equation for λ as

$$\lambda^2 + \left(1 - \frac{\alpha}{\varepsilon}\right)\lambda + \left(\frac{\beta - \alpha}{\varepsilon}\right) = 0 \quad (8)$$

From eqn. (8) we see that the temporal stability of the kinetics is determined by the function $\alpha = \alpha(f,q)$. There is a Hopf bifurcation at $\alpha = \varepsilon$, with the kinetics being stable for $\alpha < \varepsilon$ and unstable for $\alpha > \varepsilon$. Graphs of α against f for a range of values of q are shown in Fig. 1a. This figure shows that there are values f_1 and f_2 of f (which depend on q) at which $\alpha = \varepsilon$, with the system being oscillatory for $f_1 < f < f_2$ and stable and excitable for $f > f_2$. This situation is more clearly seen in the sketch shown in Fig. 1b. Fig. 1a shows that f_2 increases as ε or q are decreased.

Using the approximate expression $u_s \simeq \dfrac{(f+1)q}{(f-1)}$ for q small (and $f > 1$) derived in ref. 25, gives

$$\alpha \simeq \frac{1 + 2f - f^2}{2f}, \quad \beta \simeq 1$$

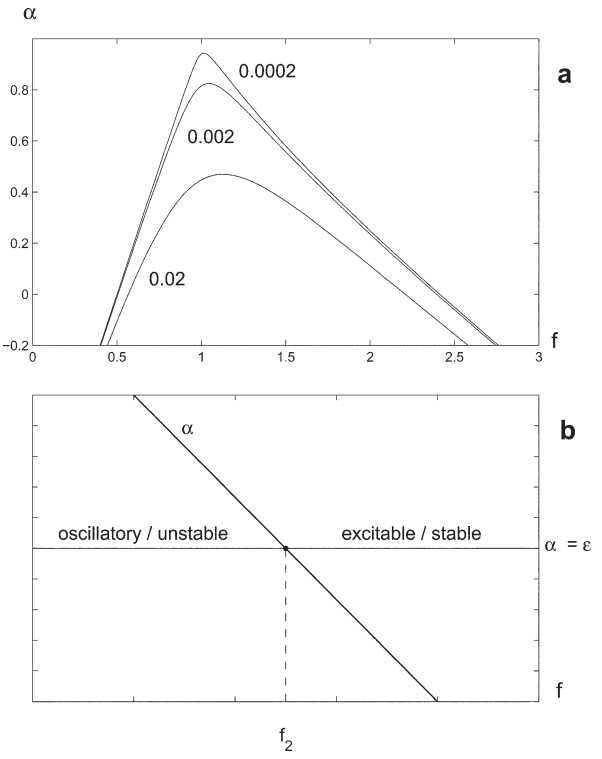

Fig. 1 (a) Plots of α against f for a range of q, the kinetic system is stable for $\alpha < \varepsilon$. (b) A sketch of α against ε to show the change from unstable (oscillatory), $\alpha > \varepsilon$, to stable (excitable), $\alpha < \varepsilon$, behaviour at $f = f_2$.

from which it follows that, for q small,

$$f_2 \simeq 1 - \varepsilon + \sqrt{2 - 2\varepsilon + \varepsilon^2} \quad (\to (1 + \sqrt{2}) \text{ as } \varepsilon \to 0)$$

3 Travelling waves

We now consider numerical solutions to the travelling wave eqns. (3) and (4) subject to boundary condition (5). We start with a brief description of our numerical method.

3.1 Numerical method

The numerical method we used is an adaptation of that described in detail in ref. 21. The basic idea behind the method is to approximate the original problem eqns. (3)–(5) with a related problem on a finite interval $[0,L]$. The zero-flux boundary conditions

$$u'(0) = w'(0) = 0, \quad u'(L) = w'(L) = 0 \quad (9)$$

are applied at the ends of the domain. Since the problem is translationally invariant we need an extra condition to fix the position of the wave. To do so, we take

$$u'(y_0) = 0 \quad (10)$$

(*i.e.* assuming that u takes its maximum value at y_0), with $0 < y_0 < L$. Previously,[21] this condition was taken at an end of the domain, the form of the concentration profiles in the present problem make it more suitable to apply it at an internal point. This constraint gives an additional equation, which we use to determine the wave speed c. Eqns. (3) and (4) are discretized on the interval $[0,L]$ and the algebraic equations that result, together with those arising from the boundary conditions (9) and the additional constraint (10), are sufficient to determine c and the values of u and w at the mesh points.

The resulting nonlinear equations were solved by Newton–Raphson iteration. As an initial starting guess we fed in a wave

profile obtained from a solution of the initial-value problem [eqns. (1) and (2)] for one set of values of f,q,ε,D. This estimate was used to start the iterative procedure to obtain a solution of [eqns. (3) and (4)], which was then continued in parameter space by a standard pseudo-arc length continuation method.[26] Checks were made on the value of L to ensure that the steady state $(u,w) = (u_s,w_s)$ was achieved with sufficient accuracy at the ends of the computational domain. We found that taking $L = 60$ (and $y_0 = 40$) was suitable for most of the parameter ranges considered.

3.2 Results

We start by giving plots of the wave speed c against f for a range of values of ε in Fig. 2a, taking $q = 0.002$, $D = 1.0$, and a plot of c against ε for $f = 2.5$, $q = 0.002$, $D = 1.0$ in Fig. 3. The main feature to note about the curves shown in Fig. 2a is the upper limit f_m on f for the existence of a solution. There is a saddle-node bifurcation in the solutions at $f = f_m$, with no travelling wave solutions for $f > f_m$ and two solutions for $f < f_m$. The value of f_m increases as ε is decreased (for given values of D and q). This feature of the solutions can also be seen in Fig. 3, for a given value of f (and D and q) there is an upper bound on ε for the existence of a travelling wave.

Fig. 2a shows that there are also lower bounds on f for the existence of travelling waves. These appear on both the upper and lower solution branches for the larger values of ε. For the smaller values of ε this appears only on the upper branch, the lower branch can be continued to $c = 0$. This feature is explained more fully in the Appendix. There we show that,

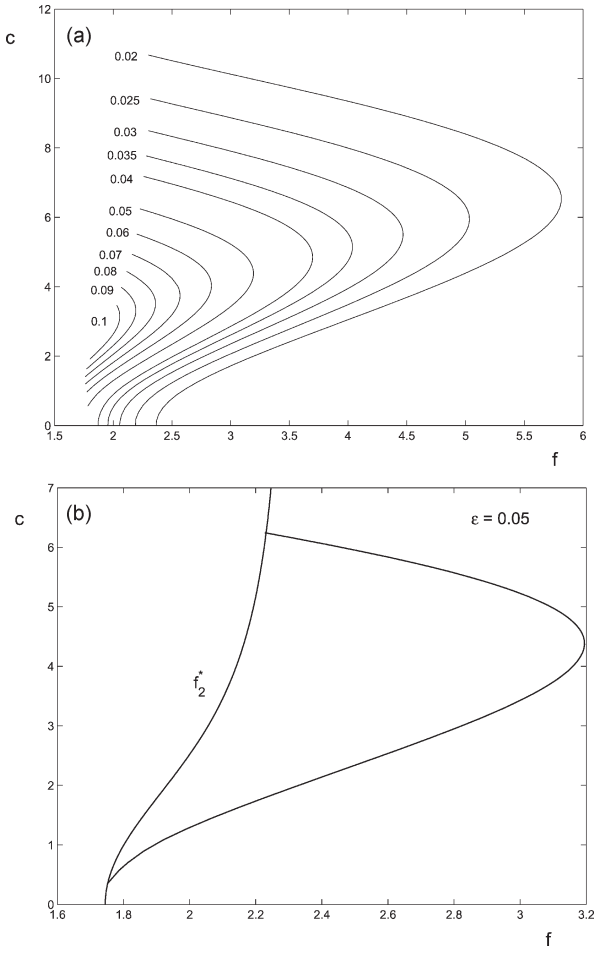

Fig. 2 (a) Plots of the wave speed c against f for a range of ε and for $q = 0.002$, $D = 1.0$. (b) Plot of f_2^*, determined from condition (19), for $q = 0.002$, $\varepsilon = 0.05$, $D = 1$. f_2^* is the limit of travelling wave solutions (also shown in the figure).

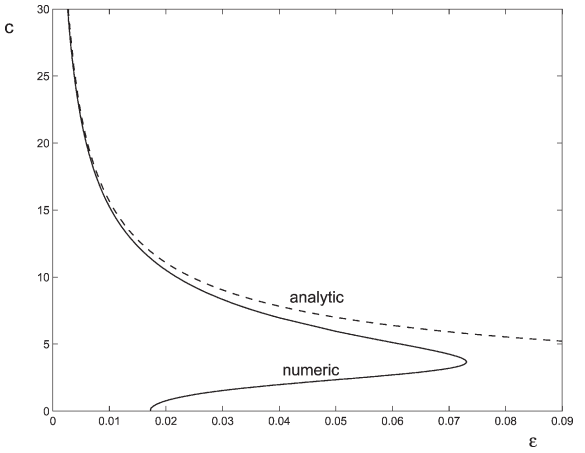

Fig. 3 Plot of the wave speed c against ε for $f = 2.5$, $q = 0.002$, $D = 1.0$ (full line). The asymptotic expression for small ε is shown by the broken line.

for given values of c, ε, D and q, there exist two values of f, f_1^*, f_2^*, such that for f values satisfying $f_1^* \le f \le f_2^*$ there are no travelling wave solutions (as single pulses). In Fig. 2b we plot f_2^* against c for $\varepsilon = 0.05$, $q = 0.002$, $D = 1$, together with the corresponding (f,c) curve (also shown in Fig. 2a). On the left-hand side of the f_2^* curve there are no travelling wave solutions, and explains why the (f,c) curve has the end points seen in Fig. 2a. We note that in the domain lying on the left-hand side of the f_2^* curve there can be wave train solutions, the existence of which we plan to investigate in the future.

An approach used previously to discuss travelling waves in excitable media is to consider the high excitability limit. The general approach to obtaining travelling wave solutions for excitable systems in the limit of high excitability has been given in ref. 15. In the present case this corresponds to obtaining a solution to eqns. (3) and (4) valid for small ε. For our Oregonator kinetics this first requires the transformation

$$\bar{y} = \varepsilon^{-1} y, \quad c = \varepsilon^{-1/2}(c_0 + O(\varepsilon)) \tag{11}$$

The leading order wave speed c_0 is then determined by the problem

$$u'' + c_0 u' + u(1-u) - \frac{f u_s (u-q)}{u+q} = 0 \tag{12}$$

on $-\infty < \bar{y} < \infty$ (primes now denote differentiation with respect to $\bar{y}$), subject to

$$u \to u_s \text{ as } \bar{y} \to \infty, \quad u \to u_0 \text{ as } \bar{y} \to -\infty \tag{13}$$

where u_0 is a zero of the kinetics of eqn. (12) and is given by

$$u_0 = \frac{1}{2}\left(1 - q - u_s + \sqrt{(1-q-u_s)^2 - 4fq}\right) \tag{14}$$

Eqn. (12), subject to eqn. (13), has to be solved numerically. This is most easily done by writing it as a first-order equation for u' in terms of u. An examination of the equilibrium points $(u_s,0)$ and $(u_0,0)$ in the (u,u') phase plane shows that they are both saddle points. Thus the required solution is a saddle–saddle connection, giving a unique value for c_0 for given values of the other parameters. The results for $q = 0.002$ are shown in Fig. 4 with a plot of c_0 against f. The computations show that c_0 decreases slowly as f increases. No upper bound on f was found (the computations were carried on to higher values of f shown in Fig. 4). For $f = 2.5$ we found that $c_0 = 1.5651$, giving $c \sim 1.5651\varepsilon^{-1/2}$ as $\varepsilon \to 0$. This expression is also plotted on Fig. 3 (by the broken line), showing good agreement with the numerical integrations for the full system even for moderate values of ε. The results for $q = 0.0008$ are also given in Fig. 4, showing that c_0 increases (for a given value of f) as q is

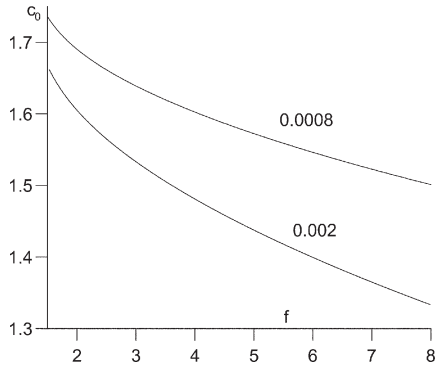

Fig. 4 The leading order wave speed c_0 obtained from the asymptotic solution for small ε, given by eqns. (12) and (13), plotted against f for $q = 0.002$ and $q = 0.0008$.

decreased. Finally, we note that these results for the asymptotic wave speed c_0 are independent of D.

We can use this result to obtain an estimate of the wave speed in terms of the initial concentrations of the reactants. In dimensional terms, the asymptotic wave speed is given by

$$v = c_0\{Dk_5[\mathrm{H^+}][\mathrm{BrO_3^-}]\}^{1/2}$$

where k_5 is the rate coefficient for the autocatalytic step in the FKN scheme.[3,4] Substituting the appropriate values for k_5 and D, this gives

$$v = 0.03c_0\left\{\frac{[\mathrm{H^+}][\mathrm{BrO_3^-}]}{M}\right\}^{1/2} \qquad (15)$$

where v is in cm s^{-1} and M is in mol dm^{-3}. This result is consistent with the simple 'Fisher-type' analysis based purely on a quadratic autocatalytic feedback of BZ waves (for which $c_0 = 2$). The dependence of the coefficient c_0 on q and f indicates how this form is modified for the actual feedback processes in the Oregonator model. In fact, c_0 is a relatively insensitive function of q and f, as shown in Fig. 4. Taking $c_0 = 1.6$ as representative, eqn. (15) becomes

$$v \approx 0.5\left\{\frac{[\mathrm{H^+}][\mathrm{BrO_3^-}]}{M}\right\}^{1/2}.$$

3.3 Limit of travelling waves, the saddle-node bifurcation

The upper limit $f_m = f_m(q,\varepsilon,D)$ on f for the existence of travelling wave solutions is, perhaps, the most significant feature to emerge from our numerical integrations. This feature, the saddle-node bifurcation in the solutions to the travelling wave equations, does not appear in the solutions obtained in the small ε limit. We now discuss this aspect in more detail. We are able to compute f_m for varying ε by writing eqns. (1) and (2) in terms of t and the travelling co-ordinate y, linearizing about the travelling wave solution and looking for a solution of the resulting equations, which has a zero temporal eigenvalue (giving the saddle-node bifurcation). This determines f_m in terms of the other parameters. The results for $q = 0.002$, $D = 1.0$ are shown in Fig. 5a with a plot of f_m against ε. Also shown in this figure (by the broken line) is f_2, the position of the Hopf bifurcation in the kinetic system. This figure shows that f_m increases as ε is decreased, with f_m becoming large for very small values of ε. This is in line with the small ε solution (described briefly above), which does not have an upper bound on f for existence. For larger values of ε, the curve crosses the Hopf bifurcation curve (at $\varepsilon = 0.0867$ for these parameter values). For higher values of ε there are no travelling wave solutions in the excitable parameter range.

We next consider the effect that changing the parameters D and q has on the limit f_m of the travelling wave solutions.

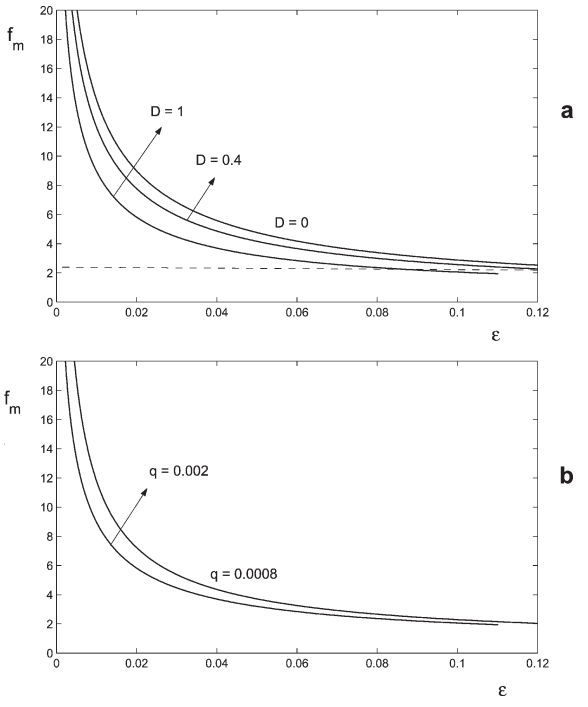

Fig. 5 Plots of f_m, the maximum value of f for which travelling wave solutions exist, against ε for (a) $D = 0.0$, 0.4, 1.0 with $q = 0.002$. The position of the Hopf bifurcation in the kinetic system at f_2 is shown by the broken line. (b) For $q = 0.0008$, 0.002 with $D = 1.0$.

We start with the ratio of diffusion coefficients. The values for the diffusion coefficients of $HBrO_2$ and ferriin given in ref. 27 for example, suggest a value for $D \simeq 0.4$. Some numerical simulations assume that M_{ox} is immobile, modelling it being fixed in a gel, see refs. 7,12 and 14 for examples. This corresponds to taking $D = 0$ in eqns. (3) and (4). Both these cases were considered and the corresponding plots of f_m against ε are also shown in Fig. 5a (all for $q = 0.002$). The figure shows that f_m increases (for a given value of ε) as D is decreased. Thus the range of existence of travelling waves increases as the diffusion coefficient of M_{ox} is reduced relative to that of $HBrO_2$.

Alternative values for the parameter q have been suggested for the Oregonator model and, to examine the effect of changing this parameter, we calculated f_m for $q = 0.0008$ to compare with the results for $q = 0.002$ (both with $D = 1.0$). Plots of f_m against ε for these two cases are shown in Fig. 5b. The figure shows that f_m is larger for the smaller value of q, with the difference between the two cases becoming a less significant as ε is increased.

4 Discussion

The saddle-node nature of the bifurcation at f_m is clearly seen when we consider the pulses that arise in the initial-value problem, eqns. (1) and (2). We integrated these equations numerically starting with u and w in their spatially uniform states (6) with u raised to an above-threshold value in a small region. The pulses that formed were monitored by plotting their propagation speed $c(t)$ against t. Results for $q = 0.002$, $\varepsilon = 0.05$, $D = 1.0$ are shown in Fig. 6 for various values of f. In this case $f_m = 3.1946$ and for $f < f_m$ (results for $f = 2.5$ and $f = 3.0$ are shown in the figure) the wave speed rapidly approaches that given on the upper branch in Fig. 2a, suggesting that this is the stable branch. For $f > f_m$, a pulse starts to develop, propagates for a while with a slowly decreasing speed before dying out rapidly as $c(t) \to 0$. The length of time that a pulse exists decreases quite quickly as f increases from f_m. For values of

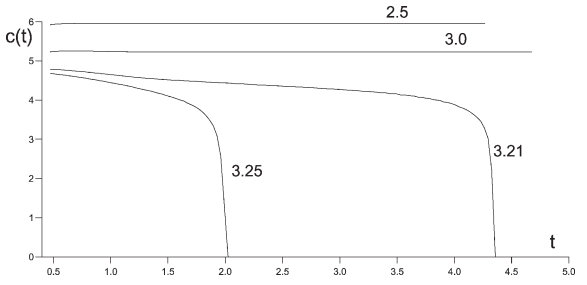

Fig. 6 Plots of the propagation speed $c(t)$ of pulses arising in numerical integrations of eqns. (1) and (2) for $q = 0.002$, $\varepsilon = 0.05$, $D = 1.0$ and $f = 2.5$, 3.0, 3.21, 3.5. Here $f_m = 3.1946$.

f just above f_m, pulses can exist for relatively long times, much longer times than are required for a pulse for $f < f_m$ to form, compare the plots for $f = 3.0$ and $f = 3.21$ in Fig. 6. An integration with $f = 3.20$ (not plotted in the figure) showed that a pulse existed until $t \simeq 7.71$. This indicates the difficulty in locating f_m exactly from numerical integrations of the initial-value problem.

Further numerical integrations of eqns. (1) and (2) have been performed for other values of ε and $f < f_m$ and in all these cases it was the pulses on the upper solution branch that developed at large times. This suggests that this is the stable branch and that the lower branch solutions are temporally unstable. As part of our numerical integrations of the travelling wave eqns. (3) and (4) we computed the temporal eigenvalues (with largest real part). These calculations confirmed that the upper branch was stable and the lower branch unstable, at least for the range of parameters considered. Coupled with this is the possibility that the upper branch solutions may lose temporal stability through a Hopf bifurcation. This change in stability has been seen in piecewise linear models[18] and might be expected to arise in the present model. However, in our numerical integrations of eqns. (3) and (4) we were unable to find this bifurcation for the upper branch solutions. We did find solutions with complex eigenvalues but their real parts were negative in all cases. This does not preclude a Hopf bifurcation occurring but it does suggest that it will require a much fuller numerical search. The numerical integrations we have performed show that, when a single pulse exists on the upper branch, *i.e.* $f_2^* < f < f_m$, this is a temporally stable solution and will be the solution that develops in the initial-value problem eqns. (1) and (2) from a single, above-threshold initial perturbation.

For all our numerical solutions we found that $f_2^* < f_2$, *i.e.* the lower bound on f for solutions on the upper branch to exist was in the oscillatory region for the kinetics. We are unable to establish this directly from eqns. (19) and (20), mainly because these involve the wave speed c, which has to be computed. We performed some integrations of the initial-value problem eqns. (1) and (2) for $f < f_2^*$ (in the oscillatory region) and found that in all cases a wave train developed from a single initial perturbation. For smaller values of ε we were able to continue the lower branch to $c = 0$ (and smoothly to negative values of c since $c = 0$ did not give a singularity in the solution). Thus there are single stationary pulse solutions to eqns. (3) and (4), though all these appear to be unstable solutions of the system (1) and (2).

One application where Oregonator kinetics are extensively used is to model the change from excitable to subexcitable regimes seen experimentally in light-sensitive BZ systems, see refs. 13, 14 and 23 for examples. The effect of applying light of (dimensionless) intensity ϕ results (ref. 14) in the modification of eqn. (3) to

$$u'' + cu' + \frac{1}{\varepsilon}\left(u(1-u) - \frac{(fw+\phi)(u-q)}{(u+q)}\right) = 0 \qquad (16)$$

This changes the steady states (now determined from a cubic equation) but does not give rise to any additional complications for our numerical method. To illustrate the effect of ϕ on the travelling waves that can form in this system, we took $q = 0.002$, $f = 2.5$ and $D = 0$ (following ref. 23) and computed solutions for $\varepsilon = 0.04$ and 0.05. The results, plots of the wave speed c against ϕ, are shown in Fig. 7. These results show that there is an upper limit ϕ_m on ϕ for the existence of a solution, with the change from excitable (pulses exist) to subexcitable (propagation failure) again being through a saddle-node bifurcation. The range of ϕ for which waves are possible increases as ε is decreased, $\phi_m = 0.03401$ for $\varepsilon = 0.05$ and $\phi_m = 0.04332$ for $\varepsilon = 0.04$. Our numerical integrations indicate that the upper bound on ϕ for solutions is quite sensitive to the choice of ε. In ref. 23 they considered the minimum light intensity necessary to excite a wave from an initial perturbation of a given radius in a two-dimensional system. Our results for ϕ_m give a lower bound for this and correspond to excitation from a region with a relatively large radius.

Finally, we comment on how the dimensionless parameters in the model can be connected to experimental conditions. In experimental terms, we can change the value of the parameter ε through the ratio of the initial malonic acid and bromate ion concentrations and by varying the pH ($\varepsilon \propto [MA]/[BrO_3^-][H^+]$). Systems with a higher 'reducing capacity' have a higher ε. The parameter q is simply a ratio of rate coefficients and so cannot be varied by changing the initial reactant concentrations (although it can be varied by changing the operating temperature). The parameter f is defined in the Oregonator model as the number of bromide ions produced in Process C for every two oxidised redox catalyst ions reduced. It is not easy to relate this parameter quantitatively to the initial reactant concentrations, although it is related to the ratio of bromomalonic acid to malonic acid. Systems with higher f can be achieved by increasing the the initial concentration of Br^- ensuring a higher initial bromination of the oxidisable organic species. It is also expected that f will increase during the long-time course of the reaction.

Appendix

Here we show that, for f values in a certain interval, there are no travelling wave solutions. To explain this feature, consider the travelling wave eqns. (3) and (4) in (u,u',w,w') phase space. The point $(u_s,0,w_s,0)$ is then an equilibrium point and a travelling wave solution corresponds to a homoclinic orbit on this point. A necessary condition for the existence of a homoclinic orbit is that the stable and unstable manifolds of the equilibrium point must both be at least one-dimensional, *i.e.* a

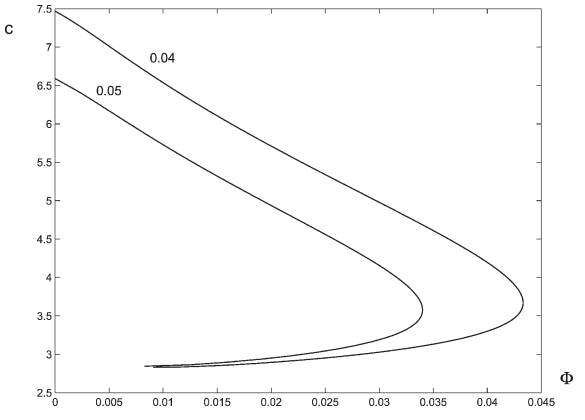

Fig. 7 Plots of the wave speed c against the light intensity ϕ for $\varepsilon = 0.004$, 0.005 and $q = 0.002$, $f = 2.5$, $D = 0$, obtained from numerical integrations of eqns. (4) and (16).

sufficient condition for the non-existence of a travelling wave is that the four eigenvalues of the Jacobian evaluated at $(u_s,0,w_s,0)$ all have a positive or a negative real part. From eqns. (3) and (4) the equation for the eigenvalues λ is, assuming that $D \neq 0$,

$$D\lambda^4 + c(1+D)\lambda^3 + \left(c^2 + \frac{D\alpha}{\varepsilon} - 1\right)\lambda^2 + c\left(\frac{\alpha}{\varepsilon} - 1\right)\lambda + \left(\frac{\beta - \alpha}{\varepsilon}\right) = 0 \quad (17)$$

This reduces to a cubic in λ when $D = 0$.

Since the coefficient of λ^3 is non-negative, eqn. (17) must have at least one root with a non-positive real part. Hence, to determine conditions for non-existence we need to consider the case when eqn. (17) has only roots with negative real parts. From the Routh–Hurwitz criterion this can happen if and only if all the following conditions hold.

$$c > 0, \quad (\beta - \alpha) > 0 \quad (18)$$

$$c[c^2(1+D)\varepsilon + D^2\alpha + D(\alpha - \varepsilon) - \alpha] > 0, \quad (19)$$

$$c^2[(\alpha - \varepsilon)(c^2(1+D)\varepsilon + D^2\alpha + D(\alpha - \varepsilon) - \alpha) - (\beta - \alpha) \times (1+D)^2\varepsilon] > 0 \quad (20)$$

Clearly the conditions in (18) always hold so that it is (19) and (20) that give the conditions for non-existence of travelling wave solutions. For given values of c, ε, D and q we can plot the left-hand side of inequalities (19) and (20) against f. These graphs are similar to those shown in Fig. 1a, having two zeros. Hence, for given values of the other parameters, there are values $\bar{f}_1$, $\bar{f}_2$, f_1^*, f_2^* of f such that inequality (19) holds when $f \in (\bar{f}_1, \bar{f}_2)$, and inequality (20) holds when $f \in (f_1^*, f_2^*)$. For the parameter ranges considered we found that $(f_1^*, f_2^*) \subset (\bar{f}_1, \bar{f}_2)$, so that it is condition (20) that gives the sufficient condition for non-existence of a travelling wave solution. That is for f values satisfying $f_1^* \leq f \leq f_2^*$ there cannot be travelling wave solutions.

Acknowledgements

We wish to acknowledge the suport of the ESF Programme REACTOR and IZK wishes to thank ORS and the University of Leeds for financial support.

References

1 R. J. Field and R. M. Noyes, *Faraday Symp. Chem. Soc.*, 1974, **9**, 21–27.
2 P. Ruoff, *Chem. Phys. Lett.*, 1982, **90**, 76–80.
3 R. J. Field, E. Körös and R. M. Noyes, *J. Am. Chem. Soc.*, 1972, **94**, 8649–8664.
4 R. J. Field and R. M. Noyes, *J. Chem. Phys.*, 1974, **60**, 1877–1884.
5 J. J. Tyson, *J. Phys. Chem.*, 1982, **86**, 3006–3012.
6 J. J. Tyson and P. C. Fife, *J. Chem. Phys.*, 1980, **73**, 2224–2237.
7 M. Gomez-Gesteira, G. Fernandez-Garcia, A. P. Munuzuri, V. Perez-Munuzuri, V. I. Krinsky, C. F. Starmer and V. Perez-Villar, *Physica*, 1994, **D 76**, 359–368.
8 J. Mosquera, M. Gomez-Gesteira, V. Perez-Munuzuri, A. P. Munuzuri and V. Perez-Villar, *Chaos*, 1995, **5**, 797–807.
9 J. J. Taboada, A. P. Munuzuri, V. Perez-Munuzuri, M. Gomez-Gesteira and V. Perez-Villar, *CHAOS*, 1994, **4**, 519–524.
10 B. Schmidt and S. C. Muller, *Phys. Rev. E*, 1997, **55**, 4390–4393.
11 H. J. Krug, L. Pohlmann and L. Kuhnert, *J. Phys. Chem.*, 1990, **94**, 4862–4866.
12 O. Steinbock, V. Zykov and S. C. Muller, *Nature*, 1993, **366**, 322–324.
13 S. Kadar, J. Wang and K. Showalter, *Nature*, 1998, **391**, 770–772.
14 I. Sendina-Nadal, E. Mihaliuk, J. Wang, V. Perez-Munuzuri and K. Showalter, *Phys. Rev. Lett.*, 2001, **86**, 1646–1649.
15 J. P. Keener, *SIAM J. Appl. Math.*, 1980, **39**, 528–548.
16 J. J. Tyson and J. P. Keener, *Physica*, 1998, **D32**, 327–361.
17 J. D. Dockery, J. P. Keener and J. J. Tyson, *Physica*, 1988, **D30**, 177–191.
18 D. A. Kessler and H. Levine, *Phys. Rev. A*, 1990, **41**, 5418–5430.
19 E. P. Zemskov, V. S. Zykov, K. Kassner and S. C. Muller, *Nonlinearity*, 2000, **13**, 2063–2076.
20 P. L. Simon, S. Kalliadasis, J. H. Merkin and S. K. Scott, *J. Math. Chem.*, 2002, **31**, 3133–332.
21 P. L. Simon, S. Kalliadasis, J. H. Merkin and S. K. Scott, *IMA J. Appl. Math.*, 2003, **68**, 537–562.
22 P. L. Simon, S. Kalliadasis, J. H. Merkin and S. K. Scott, *IMA J. Appl. Math.*, in press.
23 E. Mihaliuk, T. Sakurai, F. Chirila and K. Showalter, *Faraday Discuss.*, 2001, **120**, 383–394.
24 S. K. Scott, *Chemical chaos*, Clarendon Press, Oxford, 1991.
25 J. A. Leach, J. H. Merkin and S. K. Scott, *Philos. Trans. R. Soc. London*, 1993, **A345**, 229–258.
26 W. J. F. Govaerts, *Numerical methods for bifurcations of dynamical equilibria*, SIAM, Philadelphia, PA, 2000.
27 H. Sevcikova, J. Kosek and M. Marek, *J. Phys. Chem.*, 1996, **100**, 1666–1675.